frontiers | Frontiers in Energy Research

TYPE Original Research
PUBLISHED 12 January 2024
DOI 10.3389/fenrg.2023.1337205

OPEN ACCESS

EDITED BY
Zhengmao Li,
Aalto University, Finland

REVIEWED BY
Chenghao Sun,
Aalborg University, Denmark
Xu Xu,
Xi'an Jiaotong-Liverpool University, China
Dehao Qin,
Clemson University, United States

*CORRESPONDENCE
Xinrui Liu,
liuxinrui@ise.neu.edu.cn

RECEIVED 12 November 2023
ACCEPTED 26 December 2023
PUBLISHED 12 January 2024

CITATION
Chu T, Wang T, Li M, Feng J, Sun Y and Liu X (2024), Research on the collaborative management of internal and external fluctuations and optimization of power trading in multi-virtual power plants.
Front. Energy Res. 11:1337205.
doi: 10.3389/fenrg.2023.1337205

Research on the collaborative management of internal and external fluctuations and optimization of power trading in multi-virtual power plants

Tianfeng Chu[1,2], Tong Wang[2], Ming Li[1], Junbo Feng[1], Yufei Sun[1] and Xinrui Liu[1]*

[1]Department of Electrical Engineering, College of Information Science and Engineering, Northeastern University, Shenyang, China, [2]Electric Power Research Institute, State Grid Liaoning Electric Power Co., Ltd., Shenyang, China

Virtual power plants (VPPs), serving as an integration and coordination platform for energy sources, have been rapidly developed in recent years. With the rapid expansion of distributed energy sources, disturbance problems within the VPP and cluster are becoming increasingly prominent. In this study, we commence by addressing the internal fluctuations within the VPP through the construction of a source–load uncertainty model. Then, we integrate the Nash bargaining game theory, treating different VPPs as participants in the game. This approach significantly mitigates disturbances within both VPPs and the cluster through the negotiation of power trading strategies. In addition, the coordination between VPPs and their coordination with the distribution network in the network-wide interaction is considered, and an optimization algorithm for distributed electricity trading based on the alternating direction method of multipliers is proposed to solve the model. The results show that the proposed model effectively copes with the internal and external disturbances of the VPP, improves the system's ability to cope with the uncertainty risk, and reduces the operation cost.

KEYWORDS

virtual power plant, bidirectional source–load fluctuations, cooperative operation, Nash bargaining game, alternating direction method of multipliers

1 Introduction

In pursuit of the goals of "2030 carbon peak" and "2060 carbon neutral," China is accelerating the reform of its energy structure, building a clean and low-carbon energy system and improving the efficiency of renewable energy use (Han et al., 2021; Li et al., 2021; Sheng et al., 2021). This makes the power system face unprecedented challenges. One of them is the source–load fluctuation problem in both directions, mainly due to the distributed energy systems, such as solar power and wind power, whose power generation is affected by the weather and wind speed, as well as the uncertainty of the users' electricity consumption behavior, leading to a two-way fluctuation between power supply and demand (Deng et al., 2023; Gao et al., 2023; Tang et al., 2023).

Virtual power plants (VPPs) have been rapidly developed because of their advantages in meeting diversified energy demand and integrating distributed energy sources (Yin et al., 2018; Sheng et al., 2019). Integrating and coordinating distributed energy sources and

utilizing flexible energy scheduling strategies help reduce the impact of source–load fluctuations on the power system and are a key technology to cope with the problem of bidirectional source–load fluctuations (Pan et al., 2023a).

The source–load fluctuation problem has been studied by many scholars. Various forecasting methods have been developed to improve the energy utilization within the VPP, such as new energy output prediction and load prediction. A new energy prediction control technique with feedback correction and an adaptive predictive energy management strategy for the real-time optimal operation of the VPP was proposed in the work of Mohy-Ud-Din et al. (2021), but it cannot achieve the dual prediction of source and load. Appino et al. (2021) and Li et al. (2023) used stochastic models to predict renewable energy output and load, and the algorithm can obtain the optimal scheduling scheme with perfect prediction. In the work of Alabi et al. (2022), a deep learning approach for day-ahead prediction and applying a stochastic modeling approach for optimal decision making for the day-ahead scheduling of VPPs were discussed. The stochastic nature of weather and electricity consumption behavior leads to large deviations between forecasts and the actual situation, and the scheduling plan is unable to meet the demand for energy.

To address the issue of inadequate accuracy in forecasting new energy output and load, we employ game theory. This theory treats diverse energy entities as participants in a game, employing negotiations on power trading strategies to compensate for forecast deviations. The goal is to minimize the influence of power fluctuations on the VPP. A game optimization model of the VPP and other energy subjects was proposed in the work of Wang et al. (2022a) and Pan et al. (2023b), taking into account the interests of VPP operators and other energy subjects. In the work of Liu (2023), a two-layer game scheduling method for the VPP with multiple integrated energy systems (IESs) was proposed to ensure the reliable operation of the VPP and maximize the benefits of multiple IESs. However, the behavior of each subject in pursuit of maximizing its interests will harm the reduction of source–load uncertainty. Wang et al. (2022b) and Ju et al. (2022) constructed a VPP game model considering flexible demand response and electric vehicles to balance the multiple objectives of output fluctuation, competitive behaviors, and dispatch costs, which achieves energy complementarity and improves the overall operating economy. These studies focus on the competitive relationship among energy subjects; the potential for cooperation among different energy subjects is not sufficiently considered, and the inter-subject perturbation problem affected by the competitive relationship cannot be reasonably solved.

In response to the expanding scale of power systems, researchers have proposed cooperative optimization strategies for multi-virtual power plants (MVPPs) to address perturbation issues among VPPs. Zhou et al. (2018a), Ge et al. (2023a), and Cao et al. (2023) introduced cooperative game strategies for energy systems, accounting for constraints in distribution network operation, leading to enhanced stability in overall VPP operation and reduced operational costs. In the work of Liu et al. (2023), inter-VPP perturbations and various internal uncertainties were considered, proposing an MVPP optimization methodology that acknowledges the risky nature of operations. Zhou et al. (2018b) suggested a dual-compensation demand response mechanism for the operator and MVPP to balance conflicting market interests. They employed a Stackelberg game strategy for operators and MVPPs with dual-compensation demand response mechanisms, achieving optimal energy scheduling strategies for each VPP. Huang et al. (2023) solved the problem using a distributed, robust optimization method. Additionally, to safeguard participant privacy, an alternating direction method of multipliers (ADMM)-based distributionary robust optimization algorithm was utilized to address trading issues in a distributed framework. Qiu et al. (2021) explored the cooperation mode of the MVPP, establishing multi-objective individual and joint scheduling models for single and MVPPs, respectively. They applied cooperative game theory to effectively enhance the anti-disturbance capability of VPPs. Despite these advancements in MVPP systems realizing the cooperative mode of multiple entities, the issue of uncertainty in new energy output and load is insufficiently considered, limiting the improvement of system economy.

With the continual increase in distributed energy source penetration, the uncertainty in their output poses substantial challenges to the secure and stable operation of the MVPP system and its cooperative entities. Ge et al. (2023b) and Song et al. (2023) formulated a non-cooperative dynamic game model for day-ahead market optimization and trading within the MVPP, accounting for the uncertainty in renewable energy output. In the work of Yi et al. (2020), Hou et al. (2023), and Xie et al. (2023), an MVPP coalition game optimization model was proposed, addressing multiple uncertainties in the VPP and limited dispatch flexibility, thereby enhancing the comprehensive operational efficiency of the MVPP. Sabella et al. (2016) explored a three-layer non-cooperative energy trading approach among multi-interconnected multi-energy microgrids (MEMGs) in a restructured integrated energy market. Heterogeneous uncertainties arising from renewable energy sources, market prices, and electrical loads are addressed using a risk-averse stochastic programming method. Despite the consideration of uncertainties, energy trading is confined to VPPs and does not account for interactions with the distribution network. Ikpehai et al. (2019) and Zh et al. (2023) proposed a two-stage MVPP distributed coordination optimization model, considering distribution network characteristics to enhance MVPP operation stability while incorporating cooperative scheduling objectives for the distribution network. Cui et al. (2021) investigated point-to-point energy trading among multiple microgrids (MGs) under uncertainties. The paper suggests a two-level distributed optimization framework to bridge the gap between the physical power flow supervised by the distribution system operator and the logical point-to-point transactions among multiple MGs under uncertainty.

The aforementioned studies offer crucial insights into the optimal scheduling of the MVPP under source–load uncertainty. However, there is a paucity of research that comprehensively considers the bidirectional fluctuations of both the source and load, as well as disturbances between the MVPP and the distribution network. Consequently, this paper introduces a Nash bargaining game model for the MVPP that incorporates source–load uncertainty.

With regard to the lack of the above literature and in order to focus on addressing the disturbance problem within VPPs and

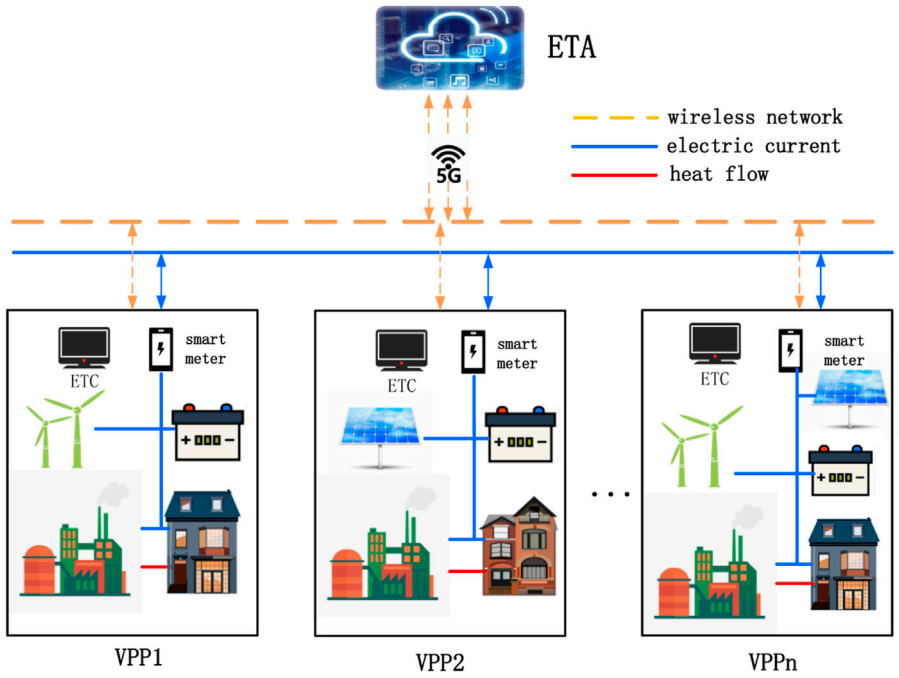

FIGURE 1
Structure of the MVPP.

clusters, this paper proposes a Nash game model for the MVPP that takes into account the source–load uncertainty. The main contributions of this paper are as follows: 1) a source load uncertainty model is formulated. By adjusting the uncertainty level to align with the specific risk preferences of each VPP, it is demonstrated that, under varying source–load fluctuations, the collaboration model enhances VPPs' capacity to manage uncertainty risks effectively. 2) A cooperative operational model for power sharing among MVPPs is formulated using the Nash bargaining theory. In this model, various VPPs are treated as participants in a game, engaging in negotiations to establish power trading strategies. This approach, combining cooperation and competition, mitigates disturbances among VPPs. 3) The ADMM is adopted to solve the optimization problem of power trading among VPPs and between them and the distribution network. Each VPP only needs to interact with the expected power trading value and power trading price information, which ensures the privacy of each VPP's information while achieving good convergence.

2 MVPP model

2.1 Structure of an MVPP

In this paper, we propose an MVPP power sharing model based on the Internet of Things technology, as shown in Figure 1. Each VPP is equipped with a smart meter device, and VPPs communicate with each other using a wireless access network (Ma et al., 2021). VPPs are internally set up with an energy trading client (ETC), which connects to the smart meter through a wireless network. The software that implements the trading function together with the smart meter and external communication is called an energy trading agent (ETA) (Wang et al., 2023). When considering privacy protection needs, the optimization strategies within each VPP can be solved locally, and only limited transaction information is exchanged through the ETA platform.

The VPP mainly consists of new energy equipment, an energy storage system, a combined heat and power (CHP) unit with a carbon capture system (CCS) and power to gas (P2G), and electric and heat flexible loads, which fully satisfy the load demand within the system through energy interaction with the higher-level grid. Each VPP within the cluster optimizes the energy price, traded power, and system unit output according to its own objectives and resource characteristics to ensure its own electric and heat load demand. The energy trading framework of this paper is shown in Figure 2.

2.2 Mathematical model of the VPP

2.2.1 CHP model with a CCS and P2G

The power model of combined heat and power is shown as follows:

$$P_{i,t}^{CHP} = V_{i,t}^{CHP} \eta_{CHP} X_{gas}, \tag{1}$$

where $V_{i,t}^{CHP}$ is the natural gas consumption, η_{CHP} is the power generation efficiency of the gas turbine, and X_{gas} is the calorific value of natural gas. Given the constraint of "electricity demand based on heat" on the CHP output of the gas turbine, the heating power of the gas turbine during period t can be delineated by the following inequality:

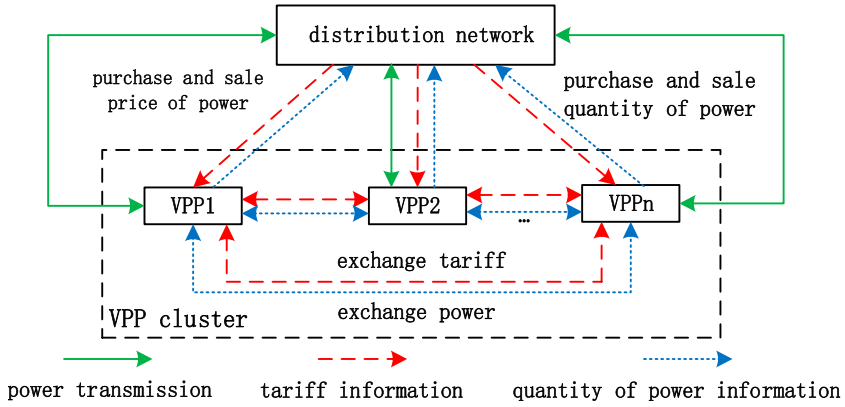

FIGURE 2
Energy trading framework.

$$\max\left\{P_{\min}-h_1H_{i,t}^{\mathrm{CHP}},h_m\left(H_{i,t}^{\mathrm{CHP}}-H_{i,0}\right)\right\}\le P_{i,t}^{\mathrm{CHP}}\le P_{\max}-h_2H_{i,t}^{\mathrm{CHP}}, \tag{2}$$

where $H_{i,t}^{CHP}$ is the heating power of the CHP unit at period t, h_1 and h_2 are the electric-heat conversion coefficients of the CHP unit corresponding to the minimum and maximum output power, respectively, h_m is the linear slope of the cogeneration power, and $H_{i,0}$ is the cogeneration power at the minimum of the CHP unit's power.

$$H_{i,t}^{GB}=V_{i,t}^{GB}\eta_{GB}X_{gas}, \tag{3}$$

$$H_{\min}^{\mathrm{GB}}\le H_{i,t}^{\mathrm{GB}}\le H_{\max}^{\mathrm{GB}}, \tag{4}$$

$$-\Delta H^{\mathrm{GB}}\le H_{i,t}^{\mathrm{GB}}-H_{i,t-1}^{\mathrm{GB}}\le\Delta H^{\mathrm{GB}}, \tag{5}$$

where $V_{i,t}^{GB}$ is the natural gas consumption of the gas turbine, η_{GB} is the heating efficiency of the gas turbine, and $H_{i,\min}^{\mathrm{GB}}$, $H_{i,\max}^{\mathrm{GB}}$, and ΔH_i^{GB} are the maximum output power, minimum output power, and maximum climbing power of gas turbine, respectively.

In the CHP model with P2G and a CCS, the generated electricity can be divided into three parts based on its utilization:

$$P_{i,t}^{CHP}=P_{i,t}^{E}+P_{i,t}^{CCS}+P_{i,t}^{P2G}, \tag{6}$$

where $P_{i,t}^{E}$ is the power supplied to meet the electricity demand of the CHP unit, $P_{i,t}^{P2G}$ is the power supplied for P2G consumption, and $P_{i,t}^{CCS}$ is the power supplied for the CCS.

The power consumption of P2G to produce natural gas is given by

$$V_{i,t}^{P2G}=\alpha P_{i,t}^{P2G}, \tag{7}$$

where α is the electrical conversion efficiency for P2G gas production.

The corresponding amount of CO_2 required for P2G is calculated using the following equation:

$$W_{i,t}^{\mathrm{CO_2}}=\beta P_{i,t}^{\mathrm{P2G}}, \tag{8}$$

where β is the coefficient for calculating the amount of CO_2.

The electric power corresponding to the CO_2 captured for P2G by the CCS is given by

$$P_{i,t}^{\mathrm{CCS}}=\gamma W_{i,t}^{\mathrm{CO_2}}, \tag{9}$$

where γ is the conversion coefficient for the consumed electric energy in capturing CO_2. The electric powers of the CCS, P2G, and the CHP should all be within their respective power limits:

$$P_{\min}^{\mathrm{CCS}}\le P_{i,t}^{\mathrm{CCS}}\le P_{\max}^{\mathrm{CCS}}, \tag{10}$$

$$P_{\min}^{\mathrm{P2G}}\le P_{i,t}^{\mathrm{P2G}}\le P_{\max}^{\mathrm{P2G}}, \tag{11}$$

$$P_{\min}^{\mathrm{CHP}}\le P_{i,t}^{\mathrm{CHP}}\le P_{\max}^{\mathrm{CHP}}, \tag{12}$$

where $P_{\min}^{\mathrm{CCS}}$ and $P_{\max}^{\mathrm{CCS}}$ are the lower and upper bounds of the electric power consumption of the CCS, respectively, $P_{\min}^{\mathrm{P2G}}$ and $P_{\max}^{\mathrm{P2G}}$ are the lower and upper bounds of the electric power consumption of P2G, respectively, and $P_{\min}^{\mathrm{CHP}}$ and $P_{\max}^{\mathrm{CHP}}$ are the lower and upper bounds of the electric power generation of the CHP, respectively.

Substituting the upper and lower constraints of Eqs. 2, (6), (10), and (11) into Eq. 13, we obtain the new coupled characteristics of CHP electric thermal power with P2G and the CCS:

$$\begin{aligned}&\max\left\{P_{\min}^{\mathrm{E}}-h_1H_{i,t}^{\mathrm{CHP}},h_m\left(H_{i,t}^{\mathrm{CHP}}-H_i^0\right)-P_{\max}^{\mathrm{P2G}}-P_{\max}^{\mathrm{CCS}}\right\}\le P_{i,t}^{\mathrm{E}}\le P_{\max}^{\mathrm{E}}\\&-h_2H_{i,t}^{\mathrm{CHP}}-P_{\min}^{\mathrm{P2G}}-P_{\min}^{\mathrm{CCS}}.\end{aligned} \tag{13}$$

2.2.2 Battery storage system model

The charging and discharging model of the battery is shown as follows.

$$E_{bat}^{t}=(1-e_{loss})E_{bat}^{t-1}+\left(P_{i,t}^{Bch}e_{bat,ec}-\frac{P_{i,t}^{Bdis}}{e_{bat,ed}}\right)\Delta t, \tag{14}$$

$$0\le P_{i,t}^{Bch}\le u_{bat}^{t}P_{max}^{Bch}, \tag{15}$$

$$0\le P_{i,t}^{Bdis}\le(1-u_{bat}^{t})P_{max}^{Bdis}, \tag{16}$$

$$E_{min}^{bat}\le E_{bat}^{t}\le E_{max}^{bat}, \tag{17}$$

$$E_{bat}^{T}=E_{bat}^{0}, \tag{18}$$

where energy loss coefficient e_{loss} <<1, P_{max}^{Bch} and P_{max}^{Bdis} are the maximum charging and discharging power, respectively, and E_{min}^{bat} and E_{max}^{bat} are the minimum and maximum storage capacity of the energy storage system, respectively.

2.2.3 Models of electrical and heating loads

The electric load at period t in the VPP consists of three parts: fixed, transferable, and curtailable electric loads, which can be expressed as follows:

$$P_{i,t}^{load} = P_{i,t}^{load_0} + P_{i,t}^{tran} + P_{i,t}^{cut}, \tag{19}$$

$$\left|\sum_{t=1}^{T} P_{i,t}^{tran}\Delta t\right| \le k^{tran} P_{i,t}^{load}, \tag{20}$$

$$0 \le P_{i,t}^{cut} \le P_{max}^{cut}, \tag{21}$$

where $P_{i,t}^{tran}$ is the transferable electric load and $P_{i,t}^{cut}$ is the curtailable electric load.

The heat load in the VPP is divided into two parts: the fixed heat load and the curtailable heat load.

$$H_{i,t}^{\text{load}} = H_{i,t}^{load_0} - H_{i,t}^{\text{cut}}, \tag{22}$$

$$0 \le H_{i,t}^{\text{cut}} \le H_{\text{max}}^{\text{cut}}, \tag{23}$$

where $H_{i,t}^{\text{cut}}$ is the curtailable heat load and $H_{i,max}^{cut}$ is the upper limit of the curtailable heat load.

2.3 Source–load uncertainty model

$$P_{i,t}^{WT} \in \left\{\hat{P}_{i,t}^{WT} - \delta_{\text{WT}}\Delta\hat{P}_{i,t}^{WT}, \hat{P}_{i,t}^{WT} + \delta_{\text{WT}}\Delta\hat{P}_{i,t}^{WT}\right\}, \tag{24}$$

$$P_{i,t}^{PV} \in \left\{\hat{P}_{i,t}^{PV} - \delta_{\text{PV}}\Delta\hat{P}_{i,t}^{PV}, \hat{P}^{PV} + \delta_{\text{PV}}\Delta\hat{P}_{i,t}^{PV}\right\}, \tag{25}$$

$$P_{i,t}^{load_0} \in \left\{\hat{P}_{i,t}^{load_0} - \delta_e\Delta\hat{P}_{i,t}^{e}, \hat{P}_{i,t}^{load_0} + \delta_e\Delta\hat{P}_{i,t}^{e}\right\}, \tag{26}$$

$$H_{i,t}^{load_0} \in \left\{\hat{H}_{i,t}^{load_0} - \delta_h\Delta\hat{H}_{i,t}^{\text{h}}, \hat{H}_{i,t}^{load_0} + \delta_h\Delta\hat{H}_{i,t}^{\text{h}}\right\}, \tag{27}$$

$$\sum_{t\in T}\delta_{\text{WT}} \le \Gamma_{\text{WT}}, \sum_{t\in T}\delta_{\text{PV}} \le \Gamma_{\text{PV}}, \tag{28}$$

$$\sum_{t\in T}\delta_e \le \Gamma_e, \sum_{t\in T}\delta_h \le \Gamma_h. \tag{29}$$

The distributed energy output, $P_{i,t}^{WT}$ and $P_{i,t}^{PV}$, and load power, $P_{i,t}^{load_0}$ and $H_{i,t}^{load_0}$, are composed of two parts: forecast value and deviation value. $\hat{P}^{WT}$, $\hat{P}_{i,t}^{PV}$, $\hat{P}_{i,t}^{load_0}$, and $\hat{H}_{i,t}^{load_0}$ denote the forecast value of distributed energy output and load power, $\Delta\hat{P}_{i,t}^{WT}$, $\Delta\hat{P}^{PV}$, $\Delta\hat{P}_{i,t}^{e}$, and $\Delta\hat{H}_{i,t}^{\text{h}}$ denote the deviation value of distributed energy output and load power, δ_{WT}, δ_{PV}, δ_e, and δ_h are binary variables, 0 means that the uncertain variables are not taken, 1 means that the uncertain variables are taken to the extremes of the uncertainty set, and Γ_{WT}, Γ_{PV}, Γ_e, and Γ_h denote the degree of uncertainty. The uncertainty modeling of the source load using this method allows a reasonable regulation of the degree of uncertainty, facilitating a comparison of the scheduling methods.

2.4 The objective function of the MVPP model

Based on the established MVPP power cooperation and sharing model, the VPP operation cost mainly consists of CHP unit operation cost, energy purchase cost, storage system operation and degradation cost, demand response cost, power transmission cost, and power sharing cost. The cost mathematical model of the VPP can be described using the following equation:

$$C_i^{VPP} = C_i^{CHP} + C_i^{w} + C_i^{ESS} + C_i^{dr} + C_i^{tran} + C_i^{net}, \tag{30}$$

where C_i^{VPP} is the operating cost of the ith VPP in the MVPP model. Each cost term is specified as follows:

1. CHP operation cost

$$C_i^{CHP} = \sum_{t=1}^{T}\left[a_1\left(P_{i,t}^{CHP}\right)^2 + b_1P_{i,t}^{CHP} + c_1\right], \tag{31}$$

where a_1 and b_1 are the operation cost coefficients of the CHP and c_1 is the operation cost constant.

2. External purchased energy cost

$$C_i^{\text{w}} = \sum_{t=1}^{T}\left[\left(\lambda_t^{buy}P_{i,t}^{buy} - \lambda_t^{sell}P_{i,t}^{sell}\right) + \lambda_{i,t}^{CH_4}V_{i,t}^{buy}\right], \tag{32}$$

where $\lambda_{i,t}^{CH_4}$ is the price of natural gas, $V_{i,t}^{buy}$ is the total gas purchased by the CHP system in period t, and λ_t^{buy} and λ_t^{sell} are the purchase and selling prices of power, respectively.

3. Operation degradation costs of the battery energy storage system

$$C_i^{\text{ESS}} = \sum_{t=1}^{T}\zeta\left(P_{i,t}^{\text{Bch}} + P_{i,t}^{\text{Bdis}}\right), \tag{33}$$

where ζ is the degradation cost per unit of charge and discharge (Britz et al., 2010).

4. Carbon quota and carbon trading cost

The carbon emission quota of the VPP is calculated using the following equation:

$$W_{i,t}^{0} = D\left(P_{i,t}^{\text{CHP}} + P_{i,t}^{PV} + P_{i,t}^{WT}\right), \tag{34}$$

where D is the carbon emission quota for the CHP VPP per unit of electricity production. The derivation of carbon trading cost is as follows:

$$C_i^{CO_2} = \sum_{t=1}^{T}\varepsilon\left(W_{i,t}^{CO_2} - W_{i,t}^{0}\right), \tag{35}$$

where ε is the carbon trading cost coefficient.

5. Demand response cost

$$C_i^{dr} = \sum_{t=1}^{T}\left(\lambda_e^{\text{cut}}P_{i,t}^{\text{cut}} + \lambda_e^{\text{tran}}P_{i,t}^{\text{tran}} + \lambda_h^{\text{cut}}H_{i,t}^{\text{cut}}\right), \tag{36}$$

where C_i^{dr} is the demand response cost and λ_e^{cut}, λ_e^{tran}, and λ_h^{tran} are the compensation unit price for the transferable and curtailable loads.

6. Power transmission cost

$$C_i^{\text{tran}} = \sum_{t=1}^{T}\sum_{j\ne i}^{\Upsilon}a_eP_{i-j,t}^{\text{net}}. \tag{37}$$

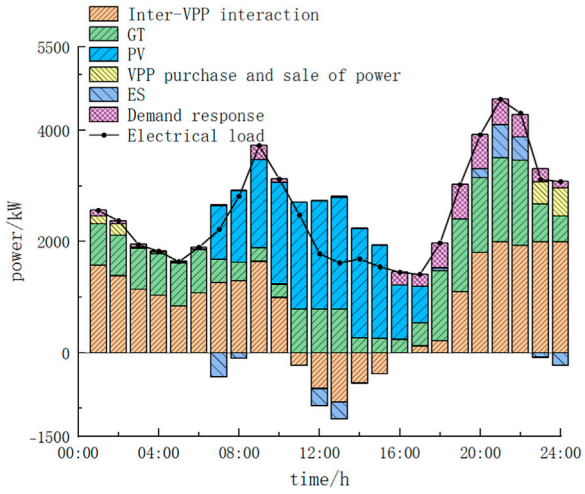

FIGURE 3
VPP2 electric power balance.

Transmission of power between VPPs necessitates the payment of a crossing charge to the distribution network operator. a_e is the crossing charge per unit of electricity. The VPP cluster is defined as Υ, where $i, j \in \Upsilon$ but $j \neq i$.

7. Power sharing cost

The power sharing cost is defined as the amount of energy trading between VPP_i and VPP_j at period t. If $P^{net}_{i-j,t} > 0$, VPP_i will obtain energy from VPP_j. Conversely, energy will be supplied to VPP_j. The price per unit of energy that needs to be paid for the amount of electricity $P^{net}_{i-j,t}$ is the power sharing cost, and the cost of energy sharing C^{net}_i is shown in the following equality:

$$C^{\text{net}}_i = \sum_{t=1}^{T} \sum_{j \neq i}^{\Upsilon} r^{\text{net}}_{i-j,t} P^{\text{net}}_{i-j,t}. \tag{38}$$

2.5 Constraints

1. Electric power balance constraint

$$P^{PV}_{i,t} + P^{WT}_{i,t} + P^{CHP}_{i,t} + P^{Bdis}_{i,t} + P^{buy}_{i,t} + P^{sell}_{i,t} = P^{load}_{i,t} + P^{Bch}_{i,t} + P^{net}_{i-j,t}. \tag{39}$$

2. Heat power balance constraint

$$H^{CHP}_{i,t} + H^{GB}_{i,t} = H^{load}_{i,t}. \tag{40}$$

3. Natural gas balance constraint

$$V^{buy}_{i,t} = V^{CHP}_{i,t} + V^{GB}_{i,t}. \tag{41}$$

4. Power trading constraint

The power output or received between VPPs at each period t should be within the limits of the transmission power limit of the wires.

$$0 \leq P^{\text{net}}_{i-j,t} \xi^{b}_{i,t} \leq P^{net}_{\max}, \forall \text{j} \in \Upsilon, \text{j} \neq \text{i}, \tag{42}$$

$$-P^{net}_{\max} \leq P^{\text{net}}_{j-i,t} \xi^{s}_{i,t} \leq 0, \forall \text{j} \in \Upsilon, \text{j} \neq \text{i}, \tag{43}$$

$$0 \leq P^{buy}_{i,t} \xi^{b}_{i,t} \leq P^{grid}_{\max}, \forall i \in \Upsilon, \tag{44}$$

$$-P^{grid}_{\max} \leq P^{sell}_{i,t} \xi^{s}_{i,t} \leq 0, \forall i \in \Upsilon, \tag{45}$$

$$\xi^{s}_{i,t} + \xi^{b}_{i,t} \leq 1, \tag{46}$$

where $P^{net}_{i,t}$ is the total amount of electricity trading by VPP_i in period t and the corresponding payment to be paid is $\nu_{i,t}$. VPPs participating in electricity trading must satisfy the energy sharing balance constraint (44) and the trading payment balance constraint (45).

$$\sum_{i \in \Upsilon} P^{net}_{i,t} = 0, \forall t, \tag{47}$$

$$\sum_{i \in \Upsilon} \nu_{i,t} = 0, \forall t. \tag{48}$$

3 Model solving of an MVPP based on Nash bargaining theory

In this study, Nash game theory and the ADMM are used to optimize the power allocation to VPPs, aiming to improve the MVPP system's ability to cope with the source–load fluctuation problem and reduce the impact of disturbances between VPPs and between them and the distribution network.

3.1 Nash bargaining theory

The Nash negotiation optimization model studied in this paper is a cooperative game, where the MVPP distributes cooperative gains among multiple participants by negotiating with each other after maximizing the benefits of the entire participating group. The Nash negotiation model satisfies a set of axioms, including symmetry and Pareto optimization. The standard Nash negotiation model is shown in equality (46). The solution that maximizes the Nash product is the equilibrium solution to the Nash negotiation game problem (Tomohiko, 2014).

$$\begin{cases} max \prod_{i \in \Upsilon} (U_i - U^0_i) \\ s.t. \quad U_i \geq U^0_i \end{cases}, \tag{49}$$

where U_i is the benefit of the negotiating subject; U^0_i is the benefit of the subject before participating in the cooperation—the point of negotiation rupture. The Nash negotiation model is a non-convex nonlinear problem, so the above model decomposition is converted into two sub-problems: the VPP cluster cost minimization sub-problem (P1) and the benefit distribution sub-problem (P2), which are solved sequentially.

3.2 MVPP model solution

To protect the privacy of each subject, P1 applies the ADMM algorithm and uses the trading power between subjects as a coupling variable to find out the optimal trading power between subjects while

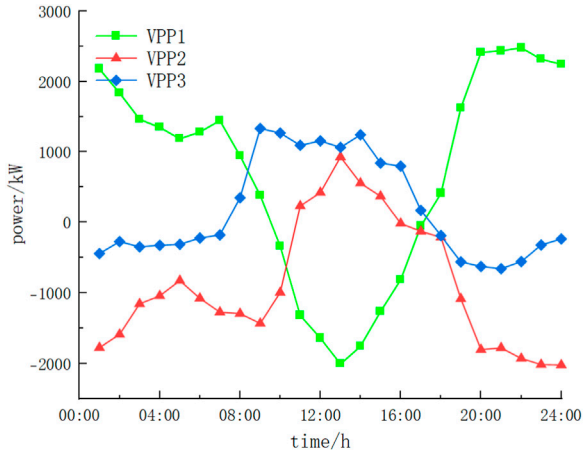

FIGURE 4
VPP cluster power trading.

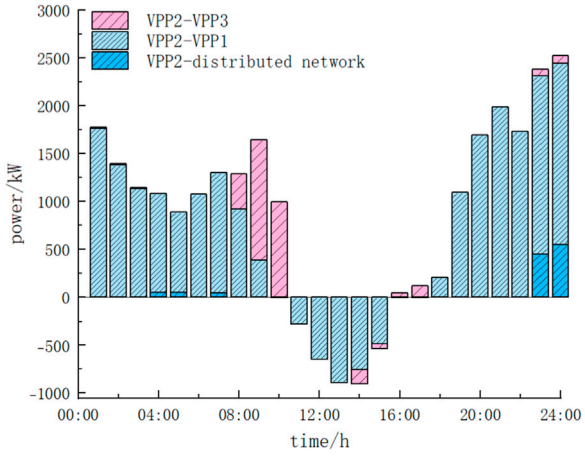

FIGURE 5
VPP2 purchase and sale of power.

simultaneously obtaining the scheduling results for each subject. P2 applies the ADMM algorithm and uses the trading price of electricity between subjects as a coupling variable to find out the optimal trading price of electricity between subjects while simultaneously obtaining the optimal revenue distribution results for each subject.

3.2.1 Solution of P1

$$\begin{cases} min\prod_{i=1}^{\Upsilon}\left[C_i^{VPP}\left(P_{i,t}^{net}\right)\right] \\ s.t.(1)-(29),(39)-(48) \end{cases}. \tag{50}$$

In the solution of P1, when the equation is satisfied, it indicates that there is a consensus on electrical power transaction between VPP_i and VPP_j.

$$P_{i-j,t}^{net}+P_{j-i,t}^{net}=0,\forall i, \tag{51}$$

where $P_{i-j,t}^{net}$ is the value of power that VPP_i expects to trade with VPP_j and $P_{j-i,t}^{net}$ is the value of power that VPP_j expects to trade with VPP_i.

The augmented Lagrange function for P1 is constructed as follows:

$$L_i^{Pl}=C_i^{VPP}+\sum_{j}^{\Upsilon}\sum_{t=1}^{T}\lambda_{i-j}^{P1}\left(P_{i-j,t}^{net}+P_{j-i,t}^{net}\right)+\sum_{j}^{\Upsilon}\frac{\rho_i^{Pl}}{2}\sum_{t=1}^{T}\parallel P_{i-j,t}^{net}+P_{j-i,t}^{net}\parallel_2^2, \tag{52}$$

where λ_{i-j}^{P1} is the Lagrange multiplier; the penalty parameter is set as $\rho_i^{P1}=10^{-4}$. The optimal traded electric power between each VPP is determined by alternatively solving equalities (50)–(52) using the ADMM.

$$P_{i-j,t}^{net}(k+1)=\mathrm{argmin}L_i^{P1}\left(\lambda_{i-j}^{P1}(k),P_{i-j,t}^{net}(k),P_{j-i,t}^{net}(k)\right), \tag{53}$$

$$P_{j-i,t}^{net}(k+1)=\mathrm{argmin}L_j^{P1}\left(\lambda_{j-i}^{P1}(k),P_{i-j,t}^{net}(k+1),P_{j-i,t}^{net}(k)\right), \tag{54}$$

$$\lambda_{i-j}^{P1}(k+1)=\lambda_{i-j}^{P1}(k)+\rho_i^{P1}\left(P_{i-j,t}^{net}+P_{j-i,t}^{net}\right). \tag{55}$$

3.2.2 Solution of P2

In the paper, a nonlinear function is used to quantify the contribution size of different VPPs in power sharing, and VPPs negotiate with each other according to their respective contributions as bargaining power to determine the trading price of power among them and achieve fair allocation. First, the energy supplied and the energy gained by each VPP during the participation optimization cycle are calculated to constitute a nonlinear energy mapping function to quantify the magnitude of the bargaining power of each VPP based on the contribution of participation in power sharing.

$$\begin{aligned} \Psi_i^s &= \sum_{t=1}^{T}\max\left(0,P_{i-j,t}^{net}\right) \\ \Psi_i^r &= -\sum_{t=1}^{T}\min\left(0,P_{i-j,t}^{net}\right) \end{aligned}, \tag{56}$$

$$\beta_i=e^{\Psi_i^s/\Psi_{\max}^s}-e^{-\left(\frac{\Psi_i^r}{\Psi_{\max}^r}\right)}, \tag{57}$$

where $\Psi_{\max}^{s}$ is the maximum value of supplied power in the VPP and $\Psi_{\max}^{r}$ is the maximum value of received power in each VPP. The MVPP asymmetric bargaining revenue sharing model is constructed based on the Nash negotiation model as follows:

$$\begin{cases} \max\prod_{i=1}^{\Upsilon}\left(C_i^0-C_i^{\mathrm{VPP}}+C_i^{net}\right)^{\beta_i} \\ \mathrm{s.t.}\,(38),(47) \end{cases}, \tag{58}$$

$$C_i^0-C_i^{VPP}+C_i^{net}>0, \tag{59}$$

where C_i^0 is the cost of VPP_i before power sharing. The maximum value problem is converted into a minimum value problem. Following the same procedure as in P1, the multi-coupling constraints on trade balance are decoupled to transform them into double-coupling constraints.

$$min\prod_{i=1}^{\Upsilon}-\beta_i ln\left(C_i^0-C_i^{VPP}+C_i^{net}\right), \tag{60}$$

$$r_{i-j,t}^{net}-r_{j-i,t}^{net}=0,\forall i, \tag{61}$$

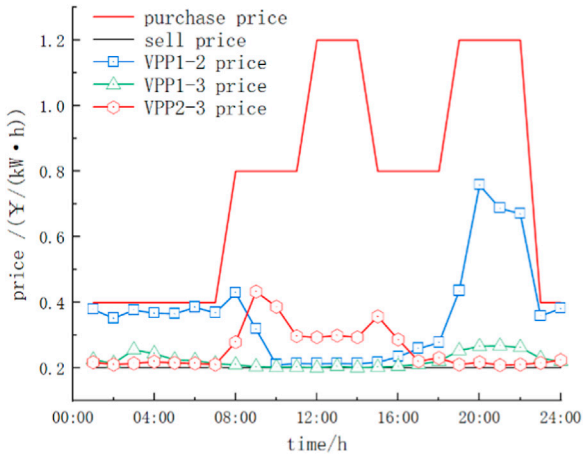

FIGURE 6
Trading price results of the VPP cluster.

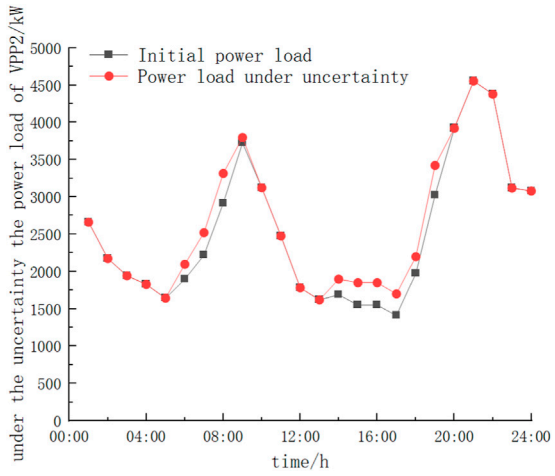

FIGURE 7
Power load of VPP2 under uncertainty.

where $r_{i-j,t}^{net}$ is the transaction price expected by VPP_i for the transaction power $P_{i-j,t}^{net}$ that has been solved in P1, $r_{j-i,t}^{net}$ is the transaction price expected by VPP_j, and $r_{i-j,t}^{net} = r_{j-i,t}^{net}$ indicates that the two sides have reached a consensus. The specific solution steps of P2 are similar to those of P1, so there is no need to go into details here.

3.2.3 Analysis of algorithm convergence

The convergence curves of P1 and P2 of this paper's algorithm are shown in Figure A1 and Figure A2. P1 converges after 32 iterations with a computation time of 275 s. P2 converges after 24 iterations with a computation time of 138 s. The results show that this paper's distributed algorithm based on the ADMM can achieve the distributed and efficient solution to the two sub-problems while considering the privacy protection of all stakeholders.

4 Case analysis

4.1 Basic data

In this paper, we consider the problem of power sharing and trading among three VPPs: the electrical and heat loads of VPPs are shown in Figures A3A, B, the new energy unit of VPP1 is wind power, the new energy unit of VPP2 and VPP3 is photovoltaic power, and VPP2's CHP unit contains carbon capture and power-to-gas equipment. The efficiency of the equipment is assumed to be constant, and the effect of the load ratio on the efficiency is ignored. The electric and heating load predictions of each VPP are shown in Figure A3. The distributed energy output forecast is shown in Figure A4. The parameters of the main equipment are shown in Table A1, and the information about electricity prices of the grid and gas prices is shown in Table A2.

4.2 Analysis of results

4.2.1 Optimization results for MVPP power trading

1. VPP internal power balance results

Figure 3 shows the power optimization paradigm within VPP2, representing a typical instance under the MVPP synergy architecture. VPP2 actively engages in the comprehensive power coordination and optimization process across the entire cluster. This involvement is contingent on satisfying its internal power demands first. Notably, the power production of the PV unit varies throughout the day. In the 11:00–18:00 time period, the PV unit generates power to meet local demand and can redistribute excess power to other VPPs. In contrast, during the periods of 0:00–10:00 and 19:00–24:00, when PV production capacity is limited, VPP2 initially draws power from other VPPs and supplements any shortage through grid purchases. This collaborative model serves a dual purpose: it diminishes energy fluctuations within the system and minimizes reliance on external grid power, thereby curbing overall operational expenses. The electrical

TABLE 1 Cost analysis before and after cooperation.

Participant	Bargaining factor (β_i)	Costs before cooperative operation/¥	Costs after cooperative operation/¥	Final allocated cost/¥	Value of cost reduction/¥
VPP1	2.3310	21,756.02	25,065.31	16,274.98	5,481.04
VPP2	1.1001	43,160.78	29,055.43	39,760.90	3,399.88
VPP3	0.8475	22,895.05	22,910.66	20,995.52	1,899.53
VPP cluster	—	87,811.85	77,031.40	0	10,780.45

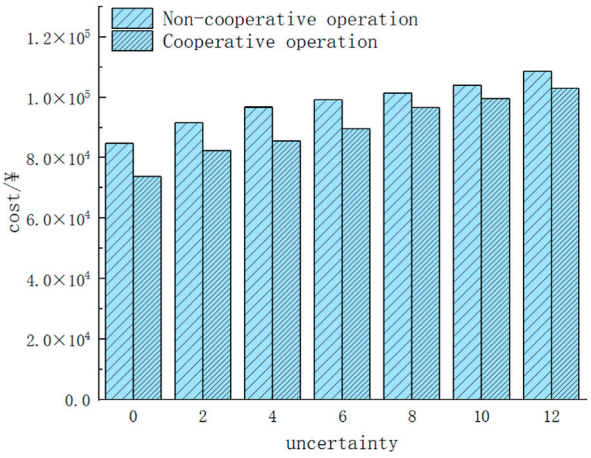

FIGURE 8
Operation cost of the MVPP with different uncertainties.

and heat power balances for the other VPPs are shown in Figures A5A, C.

2. VPP cluster power trading results

The optimization results of the electrical energy interaction of each VPP are shown in Figure 4. In the 00:00–10:00 and 16:00–24:00 time periods, the wind power production capacity in VPP1 is in surplus, which provides electrical energy for VPP2 and VPP3 to make up for the lack of electrical energy at night. On the contrary, during the 10:00–16:00 time period, the sharp increase in electric load during the daytime leads to the insufficient supply of electric energy in VPP1 when the photovoltaic power generation capacity of VPP2 and VPP3 is at its peak, in which case VPP2 and VPP3 deliver electric energy to VPP1. This complementary power sharing mechanism helps mitigate the power fluctuation among VPP clusters and improve the overall stability of the system.

3. VPP purchase and sale of power results

The external power trading of VPP2 is shown in Figure 5. When the generation equipment within VPP2 cannot meet load demand, VPP2 first purchases electric energy from other VPPs; if it still cannot meet the load demand, it considers purchasing the required electric energy from the grid. When VPP2 has excess power, it prioritizes power trading with other members in the cluster and only considers selling power to the grid if it meets the power demand of the cluster. Through this prioritized power trading strategy, the power fluctuation problem within the VPP cluster is effectively solved, ensuring that the power interaction between the VPP cluster and the distribution grid is reasonable and efficient.

4. Trading price results of the VPP cluster

The power trading price among VPPs is shown in Figure 6. It can be seen that the bargaining method is used to trade electricity between VPPs, and the electricity price is maintained within the upstream grid selling and purchasing price ranges at different periods. This strategy enables VPPs to sell electricity at a price higher than the grid purchase price and buy electricity at a price lower than the grid sale price. It increases the VPP's revenue.

4.2.2 Effects on source load uncertainty

To validate the impact of source load uncertainty and its model on the operation of the MVPP system, a case study is conducted under the following uncertainty conditions: load and wind power output uncertainties are set to 12, photovoltaic output uncertainty is set to 6, and deviation of new energy output and load power is set to 20% of the predicted values. The most adverse scenario for VPP2 under the mentioned uncertainty conditions is obtained. Taking load data as an example, the comparison analysis between the worst-case scenario and the initial predicted data is plotted in Figure 7.

From Figure 7, it can be observed that, under the consideration of uncertainty factors, the electric load power of VPP2 in the worst-case scenario is higher than the predicted values during the time periods of 06:00–08:00 and 14:00–19:00. When considering uncertainty, there is an increase in the load level, leading to a higher peak-to-valley difference and accentuating the volatility of the power load curve. To enhance the system's capability to address uncertainty factors, it is apparent that the operational costs of the VPP will increase.

To study the effect of uncertainty on the operation cost of the MVPP, seven sets of uncertainty parameters are selected to calculate the operation cost under the modes of cooperative and independent operation among the VPP members, respectively, and the results are shown in Figure 8. When the uncertainty is 2, the costs in the two modes are ¥95,760 and ¥84,689, respectively, and the cost of cooperative operation is reduced by 11. 56% based on non-cooperative operation. The cost under the cooperative mode of operation is ¥98,960 when the uncertainty is 8, which is similar to the non-cooperative operation cost of ¥99,886 when the uncertainty is 4. As the uncertainty increases, the operating cost of the system increases accordingly, but the effect of uncertainty on the operating cost can be significantly reduced by cooperative operation.

4.2.3 Cost results of the MVPP

Table 1 presents the operation cost data of each VPP before and after the cooperative operation. The results show that the cost of the VPP cluster is reduced by ¥10,780.45. Specifically, the cost of each VPP is reduced by ¥5,481.04, ¥3,399.88, and ¥1,899.53, reaching 25.19%, 7.88%, and 8.30% of the pre-cooperation cost, respectively. It shows that the cooperative game not only effectively reduces the impact of source–load fluctuations on the system but also achieves a more equitable cost distribution.

5 Conclusion

In considering the increasing percentage of distributed energy in the power system and the challenges resulting from the power system's fluctuation in distributed energy, this study introduces the Nash bargaining theory, builds a source–load uncertainty model, and uses the alternating direction method of multipliers to establish an integrated scheduling framework for a virtual power plant and its integration with the distribution network. The following are the main conclusions.

1) The constructed uncertainty model for source loads can flexibly reflect the VPP's actual risk preferences. By increasing the

uncertainty of source loads, it further intensifies the volatility of the power load curve. To enhance the system's capability to address uncertainties, there is a need to increase the operational costs of the VPP. However, adopting a cooperative game approach reveals that the total operating cost is less than the independent operation cost, effectively boosting the system's adaptability to uncertainty risks. This indicates that the strategy of collaborative cooperation not only reduces overall costs but also, while increasing flexibility, enhances the robustness of the VPP, enabling it to better adapt to dynamic environments and uncertain conditions.

2) Through cooperative operations among MVPPs, individual member costs are reduced by 25.19%, 7.88%, and 8.30%, respectively, compared to independent VPP operations. The total cost of the MVPP has decreased by 13.38%, considering both individual and collective interests. This approach effectively curtails the operational costs of the VPP.
3) The MVPP operation optimization strategy, grounded in Nash game theory, employs the ADMM algorithm for distributed solving. This algorithm facilitates the exchange of limited information on traded electricity and prices, ensuring the privacy of each participating entity, and exhibits commendable convergence properties.

In addition to the source–load fluctuation problem and the existence of perturbations among the VPP cluster, the efficiency and capacity allocation of the main equipment have some degree of influence on the cooperative operation of the MVPP. The authors intend to conduct further research on the above issues as a follow-up to this paper.

Data availability statement

The original contributions presented in the study are included in the article/Supplementary Material; further inquiries can be directed to the corresponding author.

Author contributions

TC: supervision, writing–review and editing, and conceptualization. TW: conceptualization, writing–review and editing, and investigation. ML: writing–original draft, software, and validation. JF: data curation and writing–original draft. YS: supervision and writing–review and editing. XL: supervision, writing–review, and editing, and conceptualization.

Funding

The authors declare that financial support was received for the research, authorship, and/or publication of this article. This work was supported by the Science and Technology Project of State Grid Liaoning Electric Power Supply Co., Ltd.—Research on new distribution network regulation technology considering dynamic aggregation of virtual power plant (SGLNDK00JBJS2310160).

Conflict of interest

Authors TC and TW were employed by Ltd.

The remaining authors declare that the research was conducted in the absence of any commercial or financial relationships that could be construed as a potential conflict of interest.

Publisher's note

References

Alabi, T. M., Lu, L., and Yang, Z. (2022). Data-driven optimal scheduling of multi-energy system virtual power plant (MEVPP) incorporating carbon capture system (CCS), electric vehicle flexibility, and clean energy marketer (CEM) strategy. *Appl. Energy* 314, 118997. doi:10.1016/j.apenergy.2022.118997

Appino, R., Han, W., Gonzalez, O., Faulwasser, T., Mikut, R., Hagenmeyer, V., et al. (2021). Energy-based stochastic MPC for integrated electricity-hydrogen VPP in real-time markets. *Electr. Power Syst. Res.* 195, 481–487. doi:10.1016/j.epsr.2020.106738

Britz, V., Jean, H. P., and Predtetchinski, A. (2010). Non-cooperative support for the asymmetric Nash bargaining solution. *J. Econ. Theory* 145 (5), 1951–1967. doi:10.1016/j.jet.2010.04.003

Cao, J., Yang, D., and Dehghanian, P. (2023). Co-optimization of multiple virtual power plants considering electricity-heat-carbon trading: a Stackelberg game strategy. *Int. J. Electr. Power Energy Syst.* 153, 109294. doi:10.1016/j.ijepes.2023.109294

Cui, S., Wang, Y., Liu, X., Wang, Z., and Xiao, J. (2021). Economic storage sharing framework: asymmetric bargaining-based energy cooperation. *IEEE Trans. Industrial Inf.* 17 (17), 7489–7500. doi:10.1109/TII.2021.3053296

Deng, W., Ding, L., Zhuang, Y., and Pei, W. (2023). Reachability analysis of AC/DC hybrid distribution system under uncertain disturbance. *Automation Electr. Power Syst.* 14, 52–63. doi:10.7500/AEPS20221020002

Gao, H., Guo, M., Liu, T., and Liu, J. (2023). Review on electric power and energy balance analysis of new-generation power system. *High. Volt. Eng.* (7), 2683–2696. doi:10.13336/j.1003-6520.hve.20221888

Ge, X., Cao, X., and Li, Y. (2023b). Multi-virtual power plant day-ahead stochastic game with real-time variable time scale optimization approach. *Electr. Power Autom. Equip.* 1–15. doi:10.16081/j.epae.202301003

Ge, X., Li, Y., and Yu, J. (2023a). A multi-virtual power plant optimal operation method considering risk and carbon flows. *J. Power Syst. Automation* (08), 126–135. doi:10.19635/j.cnki.csu-epsa.001152

Han, X., Li, T., Zhang, D., and Zhou, X. (2021). New issues and key technologies of new power system planning under double carbon goals. *High. Volt. Eng.* (9), 3036–3046. doi:10.13336/j.1003-6520.hve.20210809

Hou, H., Ge, X., and Cao, X. (2023). A game optimization method for multi-virtual power plant alliances considering carbon trading. *J. Power Syst. Automation* (03), 77–85. doi:10.19635/j.cnki.csu-epsa.001060

Huang, H., Li, Z., Sampath, L. P. M. I., Yang, J., Nguyen, H. D., Gooi, H. B., et al. (2023). Blockchain-enabled carbon and energy trading for network-constrained coal mines with uncertainties. *IEEE Trans. Sustain. Energy* 14 (14), 1634–1647. doi:10.1109/TSTE.2023.3240203

Ikpehai, A., Adebisi, B., Rabie, K. M., Anoh, K., Ande, R. E., Hammoudeh, M., et al. (2019). Low-power wide area network technologies for internet-of-things: a comparative review. *IEEE Internet Things J.* 6 (6), 2225–2240. doi:10.1109/JIOT.2018.2883728

Ju, L., Yin, Z., Lu, X., Yang, Sh., Li, P., Rao, R., et al. (2022). A Tri-dimensional Equilibrium-based stochastic optimal dispatching model for a novel virtual power plant incorporating carbon Capture, Power-to-Gas and electric vehicle aggregator. *Appl. Energy* 324, 119776. doi:10.1016/j.apenergy.2022.119776

Li, D., Wang, X., Shen, Y., and Jiang, D. (2023). Optimal scheduling strategy of virtual power plant with demand response and electricity-carbon trading considering multiple uncertainties. *Electr. Power Autom. Equip.* (5), 210–217. 251. doi:10.16081/j.epae.202303024

Li, H., Liu, D., and Yao, D. (2021). Analysis and reflection on the development of power system towards the goal of carbon emission peak and carbon neutrality. *Proc. CSEE* (18), 6245–6258. doi:10.13334/j.0258-8013.pcsee.210050

Liu, H., Zhao, Q., Liu, Y., Xing, Z., Hu, D., Zhang, P., et al. (2023). A multi-subject game-based operation strategy for VPPs integrating wind-solar-storage. *Sustainability* 15 (18), 6278. doi:10.3390/su15076278

Liu, X. (2023). Bi-layer game method for scheduling of virtual power plant with multiple regional integrated energy systems. *Int. J. Electr. Power* 149, 109063. doi:10.1016/j.ijepes.2023.109063

Ma, T., Pei, W., Xiao, H., Li, D., Lv, X., and Hou, K. (2021). Cooperative operation method for wind-solar-hydrogen multi-agent energy system based on Nash Bargaining theory. *Proc. CSEE* 41, 25–39. doi:10.13334/j.0258-8013.pcsee.200956

Mohy-Ud-Din, G., Kashem, M., and Sutanto, D. (2021). Adaptive and predictive energy management strategy for real-time optimal power dispatch from VPPs integrated with renewable energy and energy storage. *IEEE Trans. Industry Appl.* 57 (3), 1958–1972. doi:10.1109/TIA.2021.3057356

Pan, J., Liu, X. O., and Huang, J. (2023b). Multi-level games optimal scheduling strategy of multiple virtual power plants considering carbon emission flow and carbon trade. *Electr. Power Syst. Res.* 223 (223), 109669. doi:10.1016/j.epsr.2023.109669

Pan, M., He, X., and Ai, Q. (2023a). Status and prospects of distributed resource scheduling research for novel distribution systems. *Power Syst. Technol.* 1–16. doi:10.13335/j.1000-3673.pst.2023.0716

Qiu, G., Yu, X., Jin, L., He, C., Lou, Y., and Yang, A. (2021). Economic dispatch of regional power grids with multi-virtual power plant game. *J. Power Syst. Automation* (06), 75–83. doi:10.19635/j.cnki.csu-epsa.000481

Sabella, D., Vaillant, A., Kuure, P., Rauschenbach, U., and Giust, F. (2016). Mobile-Edge computing architecture: the role of MEC in the internet of things. *IEEE Consum. Electron. Mag.* 5 (5), 84–91. doi:10.1109/MCE.2016.2590118

Sheng, G., Qian, Y., Luo, L., Song, H., Liu, Y., and Jiang, X. (2021). Key technologies and application prospects for operation and maintenance of power equipment in new type power system. *High. Volt. Eng.* (9), 3072–3084. doi:10.13336/j.1003-6520.hve.20211258

Sheng, W., Wu, M., Ji, Y., Kou, L., Pan, J., Shi, H., et al. (2019). Key techniques and engineering practice of distributed renewable generation clusters integration. *Proc. CSEE* (8), 2175–2186. doi:10.13334/j.0258-8013.pcsee.182456

Song, J., Yang, Y., Xu, Q., Liu, Z., and Zhang, X. (2023). Robust bidding game approach for multiple virtual power plants participating in day-ahead electricity market. *Electr. Power Autom. Equip.* 43, 77–85. doi:10.16081/j.epae.202211020

Tang, W., Zhang, Q., Zhang, L., Zhang, B., and Zhang, Y. (2023). Concept, Key technologies and development direction of multilevel ac/dc interconnection in the new distribution system. *Automation Electr. Power Syst.* (6), 2–17. doi:10.7500/AEPS20221031014

Tomohiko, K. (2014). A noncooperative foundation of the asymmetric Nash bargaining solution. *J. Math. Econ.* 52 (52), 12–15. doi:10.1016/j.jmateco.2014.03.004

Wang, J., Guo, C., Yu, C., and Liang, Y. (2022b). Virtual power plant containing electric vehicles scheduling strategies based on deep reinforcement learning. *Electr. Power Syst. Res.* 205 (205), 107714. doi:10.1016/j.epsr.2021.107714

Wang, L., Wang, Zh, Li, M., and Yang, X., (2023). Distributed optimization for network-constrained peer-to-peer energy trading among multiple microgrids under uncertainty. *Int. J. Electr. Power & Energy Syst.* 149, 109065. doi:10.1016/j.ijepes.2023.109065

Wang, X., Zhao, H., Lu, H., Zhang, Y., Wang, Y., and Wang, J. (2022a). Decentralized coordinated operation model of VPP and P2H systems based on stochastic-bargaining game considering multiple uncertainties and carbon cost. *Appl. Energy* 312, 118750. doi:10.1016/j.apenergy.2022.118750

Xie, H., Yan, Q., Li, Y., Shi, Y., and Shen, Y. (2023). Distributed coordination optimization of multiple virtual power plants considering regional load characteristics in market. *Electr. Power Autom. Equip.* (43), 199–209. doi:10.16081/j.epae.202304002

Yi, Z., Xu, Y., Zhou, J., Wu, W., and Sun, H. (2020). Bi-level programming for optimal operation of an active distribution network with multiple virtual power plants. *IEEE Trans. Sustain. Energy* 11 (11), 2855–2869. doi:10.1109/TSTE.2020.2980317

Yin, S., Ai, Q., Zeng, S., Wu, Q., Hao, R., and Jiang, D. (2018). Challenges and prospects of multi-energy distributed optimization for energy internet. *Power Syst. Technol.* (5), 1359–1369. doi:10.13335/j.1000-3673.pst.2017.2849

Zh, Li, L., Wu, Y., Xu, L., and Wang, N., (2023). Distributed tri-layer risk-averse stochastic game approach for energy trading among multi-energy microgrids. *Appl. Energy* 331, 120282. doi:10.1016/j.apenergy.2022.120282

Zhou, B., Lv, L., Gao, H., Liu, J., Chen, Q., and Tan, X. (2018a). Robust day-ahead trading strategy for multiple virtual power plants. *Power Syst. Technol.* (42), 2694–2703. doi:10.13335/j.1000-3673.pst.2018.0287

Zhou, B., Lv, L., Gao, H., Liu, J., Chen, Q., and Tan, X. (2018b). Robust day-ahead trading strategy for multiple virtual power plants. *Power Syst. Technol.* (42), 2694–2703. doi:10.13335/j.1000-3673.pst.2018.0287

Appendix

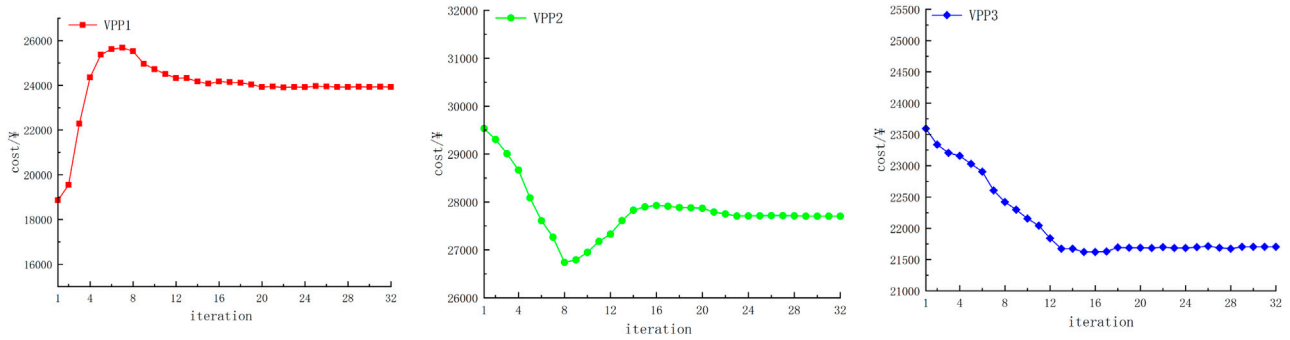

FIGURE A1
Convergence process of P1.

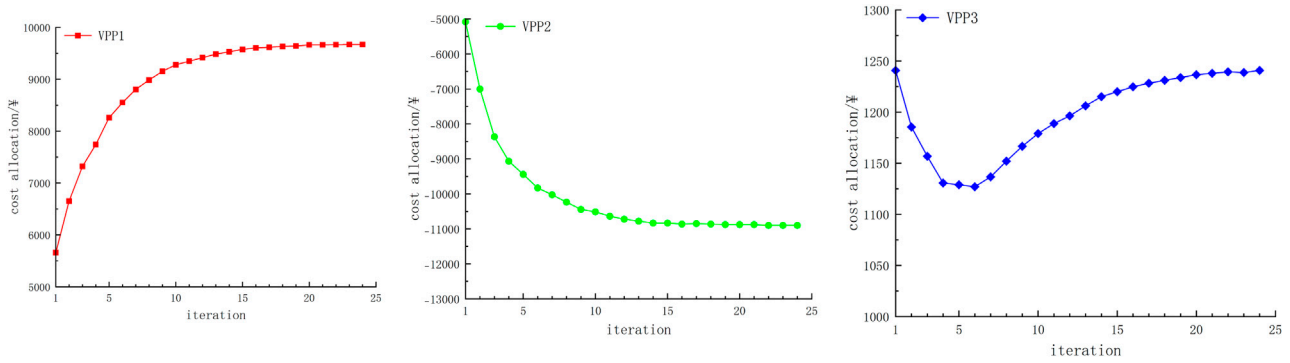

FIGURE A2
Convergence process of P2.

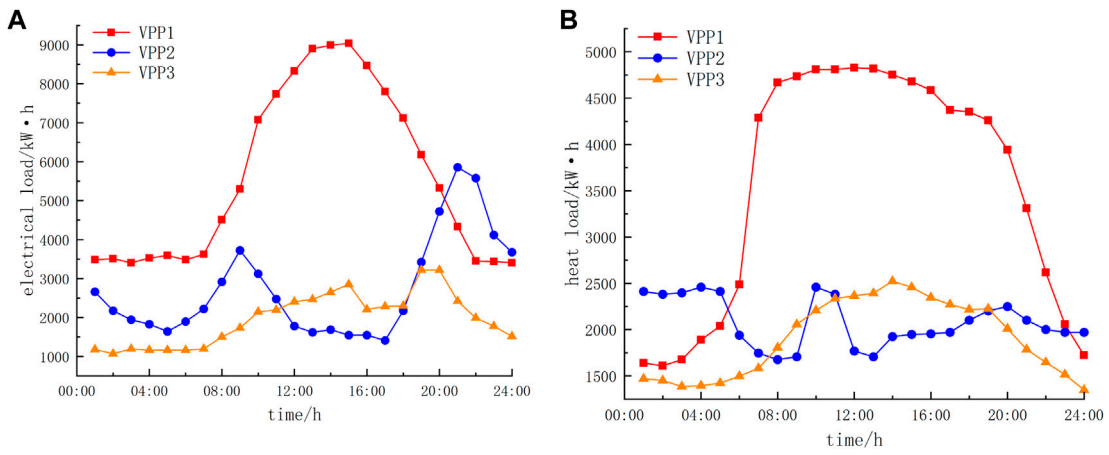

FIGURE A3
(A) Electrical load. **(B)** Heat load.

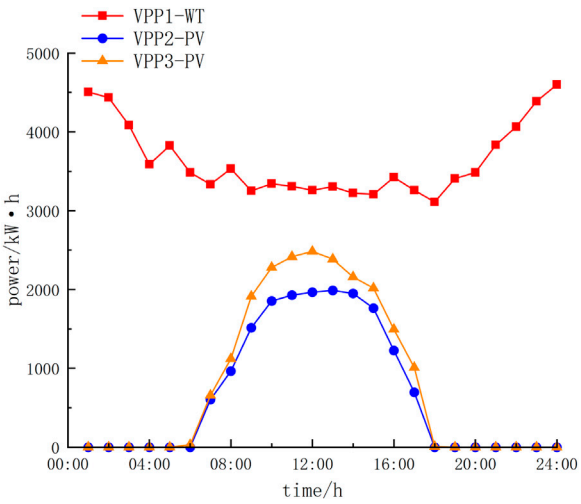

FIGURE A4
Distributed energy output forecast.

TABLE A1 VPP system parameters.

Parameter	Value	Parameter	Value	Parameter	Value
η_{CHP}	0.35	$P^{Bdis}_{\max}$/kW	500	a_1 (¥/kW)	0.01170
η_{GB}	0.85	k^{tran}	0.15	b_1 (¥/kW)	4.00×10^{-6}
X_{gas} (MJ/M^3)	35	$P_{i-j,\max}$/kW	2,000	c_1 (¥/kW)	0.02
h_1	0.155	$H^{GB}_{\min}$/kW	0	a_e (¥/kW)	0.02
h_2	0.20	$H^{GB}_{\max}$/kW	800	ζ (¥/kW)	0.015
h_m	0.85	$E^{bat}_{\min}$	500	λ^{cut}_e (¥/kW)	0.3
$P_{\min}$/kW	1,200	$E^{bat}_{\max}$	1,800	λ^{tran}_e (¥/kW)	0.1
$P_{\max}$/kW	3,200	P^{CCS}_{min}/kW	0	λ^{cut}_h (¥/kW)	0.2
$e_{bat,c}$	0.95	P^{CCS}_{max}/kW	600	α/(m^3/kW)	0.5
$e_{bat,d}$	0.95	P^{P2G}_{min}/kW	0	β/(kg/kW)	0.5
$P^{Bch}_{\max}$/kW	500	P^{P2G}_{max}/kW	300	γ/(kW·h/kg)	1.02

TABLE A2 Electricity prices of grid and gas prices.

Type	Period	Price
Electricity prices	Peak period (12:00–14:00, 19:00–22:00)	1.20 (¥/kW·h)
	Bottom period (23:00–07:00)	0.40 (¥/kW·h)
	Normal period (08:00–11:00, 15:00–18:00)	0.75 (¥/kW·h)
Natural gas price	Whole day	3.50 (¥/m^3)

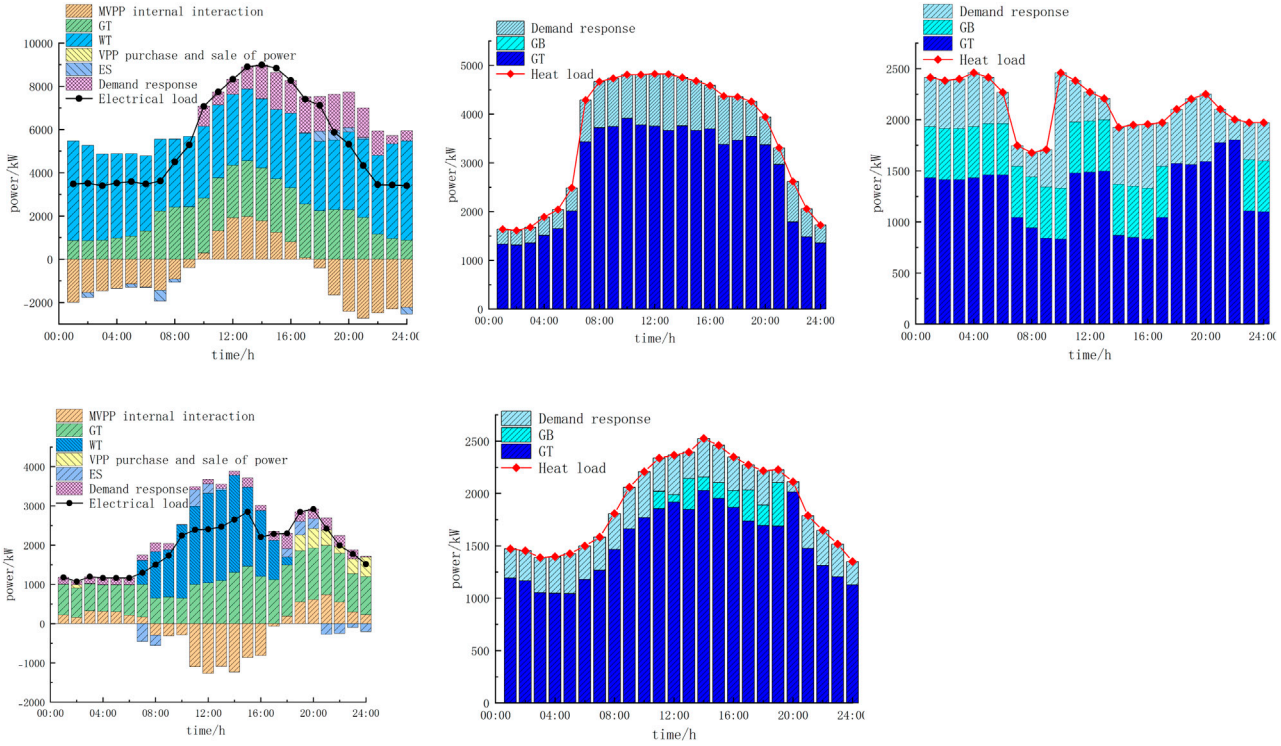

FIGURE A5
Other VPP power balance, **(A)** VPP1, **(B)** VPP2, and **(C)** VPP3.